DOI: 10.1002/ejoc.200901024

Selective Recognition of β-Mannosides by Synthetic Tripodal Receptors: A 3D View of the Recognition Mode by NMR

Ana Ardá,[a] Chiara Venturi,[a,b] Cristina Nativi,[b,c] Oscar Francesconi,[b] F. Javier Cañada,[a] Jesús Jiménez-Barbero,*[a] and Stefano Roelens*[d]

Keywords: Molecular recognition / Carbohydrates / Conformation analysis / NMR spectroscopy / Receptors

Unravelling the structural features of carbohydrate recognition by receptors is a topic of major interest. In recent years, several synthetic receptors capable of binding different sugars with moderate to good affinities and selectivities have been developed. Here we report on the analysis of the three-dimensional structures of the complexes of two recently derived synthetic tripodal receptors with octyl β-D-mannopyranoside, a monosaccharidic glycoside selectively recognized in a polar solvent, by a combination of NMR methods and assisting molecular mechanics calculations. The variations in the chemical shifts upon complexation and the observed intermolecular NOEs were employed to validate the molecular-mechanics-derived structures. The structures of the obtained complexes explain the observed mannose selectivity in chemical terms, suggesting that a combination of van der Waals, CH–π and hydrogen-bonding forces are involved in the formation of the complexes, together with stabilizing conformational effects of the substituents.

Introduction

Molecular recognition processes are at the heart of a variety of key living events. Recognition processes involving carbohydrate moieties in cellular glycoconjugates have a significant impact on different aspects of cell biology, because they serve to mediate communication between cells and their environments.[1] Decoding of the glycan signals is performed by lectins (carbohydrate-binding proteins devoid of enzymatic activity, not including antibodies and transport proteins for free glycans) and by enzymes.[2]

The selectivities and specificities of these carbohydrate–protein interactions depend on a variety of factors. Indeed, because of the amphipathic characters of sugars, different types of forces may be involved in their recognition by receptors.[3] Typically, though, carbohydrate recognition relies upon multiple weak interactions, of which hydrogen bonds (H-bonds) and van der Waals forces seem to be the most important,[4] so protein–carbohydrate interactions are relatively weak in relation to other forms of biomolecular association.[5] Furthermore, it is unclear how natural saccharide binding is achieved. Broadly speaking, there are two hypotheses. The first suggests that the interaction is essentially polar, with binding in the protein–carbohydrate complex being driven by an especially favourable set of hydrogen bonds. The second proposes that solvent reorganization is a major player. Both carbohydrates and their complementary binding sites are amphiphilic, with hydrophobic regions flanking the polar groups.

In-depth studies with natural receptors may be problematic. However, model systems based on synthetic analogues can be designed or manipulated in such a way that they are compatible with a variety of conditions. Indeed, biomimetic carbohydrate receptors[6] have been sought for modelling of natural recognition and have been exploited in different applications. Although clear selectivity has rarely been achieved with use of synthetic lectins,[7] we have recently reported on a new member of a family of tripodal receptors that specifically recognizes mannosides,[8] even in a polar solvent, with unprecedented affinity and, to the best of our knowledge, with the best selectivity for the β-mannosyl residue reported to date. Despite the prominent role of mannose in glycoscience, most synthetic receptors reported in the literature preferentially bind to glucose,[6,7] whereas receptors showing some level of preference for mannose have been rare.[9]

[a] Chemical and Physical Biology, Centro de Investigaciones Biológicas, CSIC,
Ramiro de Maeztu 9, 28040 Madrid, Spain
Fax: +34-915-360432
E-mail: jjbarbero@cib.csic.es
[b] Dipartimento di Chimica Organica, Università di Firenze, Polo Scientifico e Tecnologico,
50019 Sesto Fiorentino, Firenze, Italy
[c] Centro Risonanze Magnetiche (CERM), Polo Scientifico e Tecnologico,
50019 Sesto Fiorentino, Firenze, Italy
[d] Istituto di Metodologie Chimiche (IMC), Consiglio Nazionale delle Ricerche (CNR), Dipartimento di Chimica Organica, Polo Scientifico e Tecnologico,
50019 Sesto Fiorentino, Firenze, Italy
Fax: +39-055-4573570
E-mail: stefano.roelens@unifi.it

Supporting information for this article is available on the WWW under http://dx.doi.org/10.1002/ejoc.200901024.

In order to improve the selectivity of the recognition process further, the derivation of a 3D model for the host–guest complex is essential. We therefore describe here the structural and conformational features and geometries of the complexes formed by two of our recently derived tripodal receptors (**1** and **2**, Scheme 1) with octyl β-D-mannopyranoside (OctβMan), towards which a distinctive binding selectivity has been reported.[8] The key groups involved in the recognition have been identified and the relative orientations of the mannoside with respect to the synthetic receptors have been analysed by a combination of NMR spectroscopic data and assisting modelling calculations. In this context, it is essential to consider that for saccharides and their complexes in general, the number and distribution of the NOEs[10] might not be sufficient for full characterization of the solution conformation with reasonable certainty, especially in cases of flexible structures. If interpretation of intermolecular NOE data in terms of a unique structure is impossible, a combination of several conformations is required to avoid the generation of virtual geometries. In addition to the $1/r^6$ dependence on distance, NOEs display complex time dependence, in which the overall molecular tumbling may interact with the kinetics of the conformational or chemical exchange involved in the internal motion.

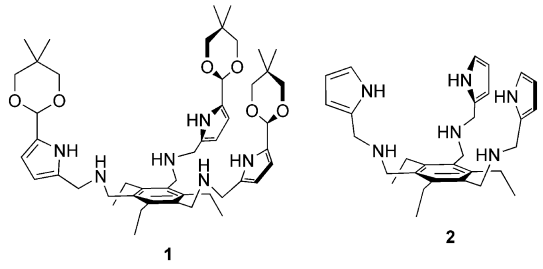

Scheme 1. Chemical structures of receptors **1** and **2**.

Results and Discussion

Comparison between the NMR spectra recorded for the free and bound species, under the experimental conditions described in the Experimental Section, showed clear and significant changes in the signals of both receptor **1** and OctβMan when they were combined in acetonitrile solution (Figure 1). The two H-3 protons of the receptor, which in the free state resonate as one single signal, for instance, become two AB systems in the presence of the mannoside. Furthermore, the two H-10 and H-12 protons appear as complex multiplets in the presence of the sugar. The largest chemical shift differences between the free and the bound states are observed for NH-5 and for H-15, which also become two different multiplets upon binding. With regard to the sugar moiety, a drastic upfield shift of nearly 1 ppm is observed for H-4 in the presence of receptor **1**, with important shielding for H-5 and the two H-6 protons. The observed high-field shift of H-3 is also noteworthy (see Tables 1 and 2).

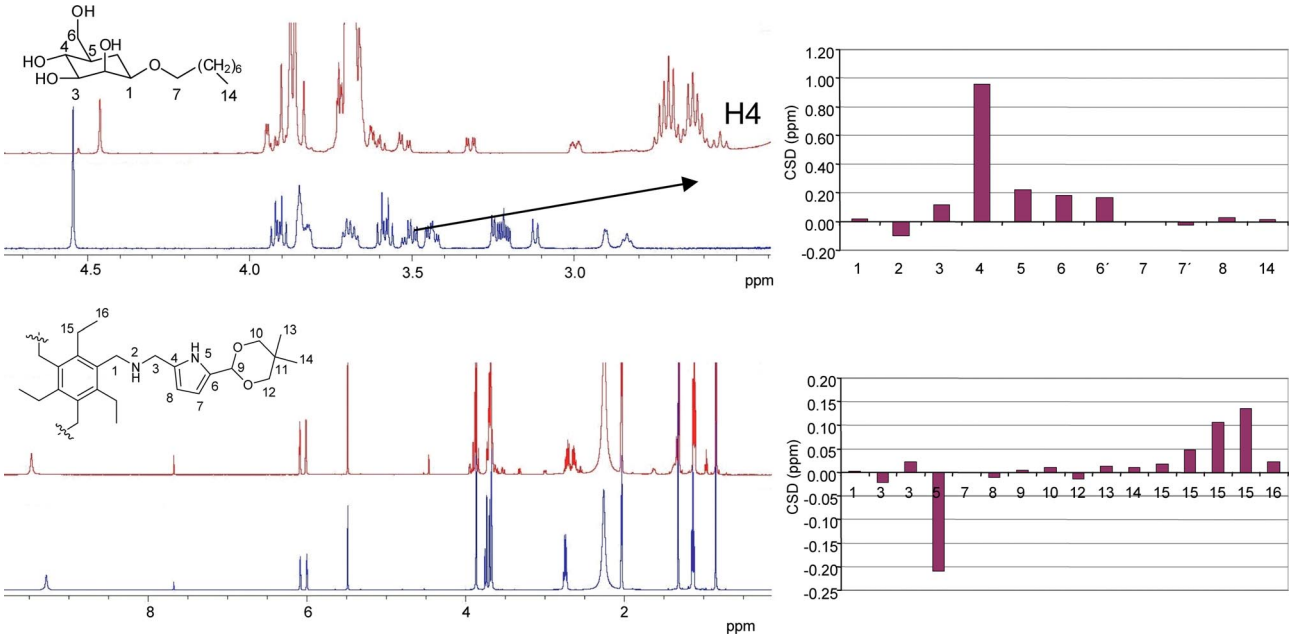

Figure 1. Left panel: 500 MHz ^{1}H NMR spectra in CD_3CN at 298 K. Top: OctβMan, neat (in blue) and in the presence of **1** (3 equiv., in red). Bottom: Compound **1** neat (in blue) and in the presence of OctβMan as above (in red). Right panel: Top: Plot of the observed CSDs of OctβMan in the presence of **1**. Bottom: Plot of the observed CSDs of **1** in the presence of OctβMan. The numbers in the graphics on the right-hand side refer to the corresponding protons in OctβMan (above) and receptor **1** (below), as shown in the scheme with the atomic numbering. The variation in the chemical shift of Man H-4 is indicated. The change in multiplicity of this signal is due to the loss of the coupling to the hydroxy proton upon binding.

Table 1. Chemical shifts (δ, ppm) and chemical shift differences (CSD, ppm) of the protons of OctβMan, free and bound to receptor **1** (CD_3CN, 298 K). The key changes are underlined. (n.o.: not observed).

Proton	Free	Bound	CSD
H-1	4.543	4.527	0.016
H-2	3.846	3.946	–0.100
H-3	3.438	3.319	0.119
H-4	3.507	2.549	*0.958*
H-5	3.215	2.995	*0.220*
H-6	3.819	3.639	0.180
H-6′	3.689	3.521	0.168
H-7	3.910	3.911	–0.001
H-7′	3.581	3.607	–0.026
H-8	1.654	1.624	0.030
H-9/H-13	1.45–1.37		
H-14	0.977	0.962	0.015
OH-2	2.901	n.o.	0.016
OH-3	3.118	n.o.	–
OH-4	3.248	n.o.	–
OH-6	2.836	n.o.	–

Table 2. Chemical shifts (δ, ppm) and chemical shift differences (CSD, ppm) of the protons of receptor **1**, free and bound to OctβMan (CD_3CN, 298 K). The key changes are underlined.

Proton	Free	Bound	CSD
H-1	3.679	3.676	0.003
H-3	3.869	3.890	–0.021
H-3	3.869	3.846	0.023
NH-5	9.258	9.467	*–0.209*
H-7	6.083	6.083	0.000
H-8	5.998	6.008	–0.010
H-9	5.485	5.481	0.004
H-10/H-12	3.732		
H-10′/H-12′	3.685		
H-13	1.319	1.305	0.014
H-14	0.848	0.838	0.010
H-15	2.748	2.730	0.018
H-15	2.748	2.700	0.048
H-15	2.748	2.641	0.107
H-15	2.748	2.612	*0.136*
H-16	1.139	1.116	0.023

Conclusive evidence for the existence of a stable complex in solution was provided by the observation of intermolecular ligand/receptor NOEs. Indeed, the following intermolecular contacts were clearly evident as cross-peaks in the NOESY map: NH-5/H2, NH-5/H-7′, NH-5/H-6′, NH-5/H-8, NH-5/H-3, CH_3-13/H-1, CH_3-13/H-2, CH_3-13/H-3 and CH_3-13/H-5 (Figure 2).

Altogether, these data seem to indicate the existence of some specific binding modes characterizing the complex of the receptor with OctβMan. Because the receptor shows a binding affinity for βMan that is at least one order of magnitude larger than that observed for other simple sugars, including αMan, α- and βGlc, α- and βGal and α- and βGlcNAc,[8] the identification of the preferred geometry of the complex in solution may open a pathway to the development of new receptors featuring enhanced affinities through structure-based design.

It should be pointed out that although binding measurements revealed multiple complex species in solution,[8] under the concentration conditions employed in this investigation the dominant species is the 1:1 complex, which accounts for over 60% of the species present in solution, with complexes of higher stoichiometry amounting to less than 20%, thus substantially determining the NMR phenomenology.

The molecular modelling protocol described in the Experimental Section was adopted for structure assessment, providing three families of structures within 9.3 kJ mol^{-1}.

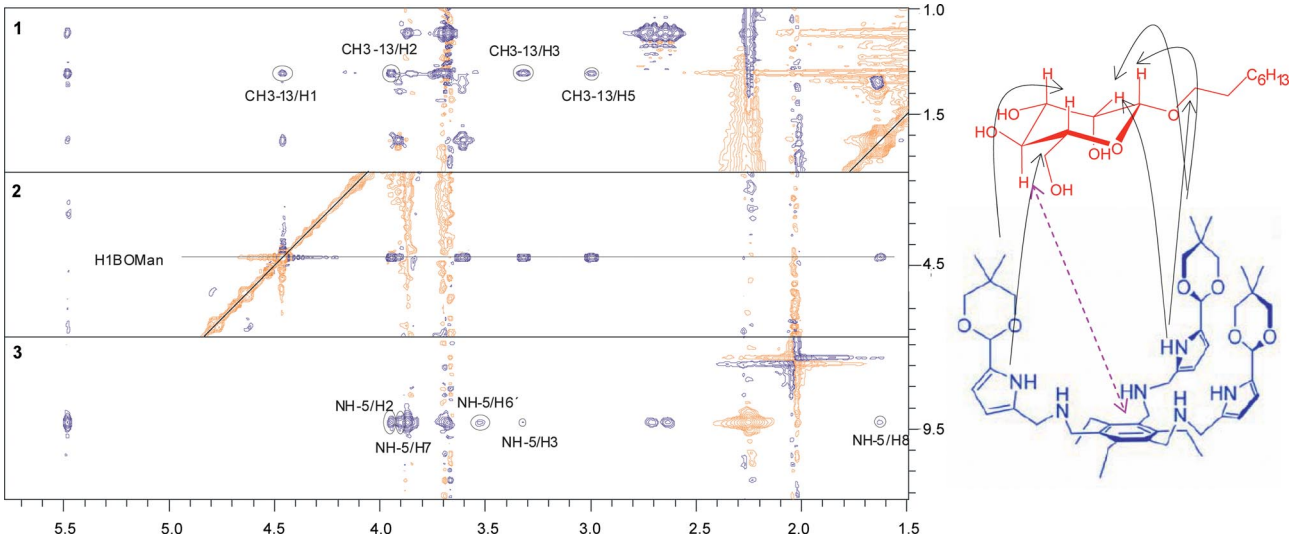

Figure 2. 500 MHz NOESY spectrum of a 1:3 mixture of OctβMan and **1** in CD_3CN at 298 K, acquired with a 500 ms mixing time. Intermolecular NOEs between the CH_3-13 and NH-5 protons of **1** and several sugar protons are indicated in the top and bottom sections, respectively. Intramolecular NOEs involving the anomeric proton of the sugar can be seen in the middle section. A schematic representation of NOE contacts is depicted.

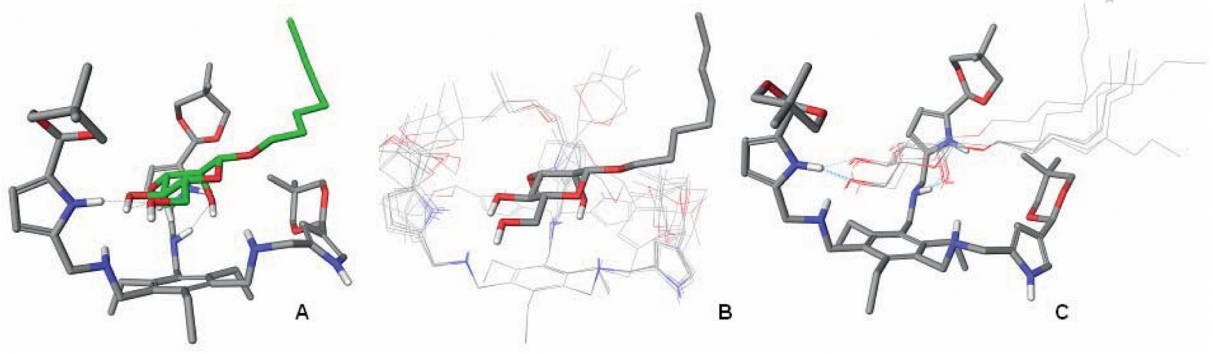

Figure 3. A) Structure of the global minimum of the 1:1 complex between **1** and OctβMan. B) Perspective from the sugar showing the orientations of the pyrrole binding arms. C) Perspective from the receptor showing the orientations of the sugar. Hydrogen bonds are depicted in dashed lines.

The lowest-energy family corresponds to the structure depicted in part A of Figure 3, including seven geometries featuring slightly different orientations of the sugar and of the "arms" ("arms" refers to the extensions containing the aminopyrrole moieties) of the tripodal receptor, as shown in parts B and C of Figure 3. These geometries were considered to correspond to the most likely NMR-based experimental solution and were further explored. Indeed, the experimentally observed dramatic shielding of the H-4 proton of OctβMan (ca. 1 ppm, Figure 1, Table 1) in the presence of the receptor strongly supports proximity of this nucleus to the centre of the benzene ring of the receptor, a feature

Table 3. Selected structural parameters (from NMR spectroscopic data and modeling calculations) and relative energies (AMBER* force field; see Exp. Sect.) of the most stable complexes of **1** with OctβMan. The best matching values between modelled and experimentally determined distances (estimated from NOEs) for different conformers are underlined. The relevant intermolecular hydrogen bonds are also reported. The intensities of the experimentally measured NOEs are given in the upper part of the Table: s: strong for >10% intensity; ms: medium-strong for 7–10% intensity; m: medium for 3–7% intensity; w: weak for 2–3% intensity; vw: very weak for <1% intensity. ov: overlapped peaks. A: amine; P: pyrrole.

					Intermolecular atom pair (**1**/OctβMan)								
					NH5/ H2	NH5/ H7	NH5/ H6′	NH5 /H3	NH5/ H8	H13/ H1	H13/ H2	H13/ H3	H13/ H5
					Experimentally measured NOE intensity								
					s	ov	w	vw	vw	m	m-s	s	m
	AMBER* calculations												
Conformer[a]	*E*[b] [kJ mol^{-1}]	*d*[c] (Å)	Intermolecular H-bonds	Intramolecular H-bonds	Distance (Å) between atom pairs for each conformer								
1	0	2.78	O(H)6–NH P O(H)2–NH A O5–NH A	OH4-O(H)6	*2.95*	5.57	*3.76*	*4.55*	*5.42*	*2.68*	*3.75*	3.54	4.69
7	4.2	2.90	O(H)2–NH A	OH4–O(H)6	*2.18*	6.3	*3.64*	3.19	*4.9*	5.2	4.64	5.16	6.17
8	4.4	2.74	O(H)6–NH P	OH4–O(H)6	3.95	3.74	*3.73*	3.89	2.70	5.75	*3.25*	4.54	5.33
9	4.7	2.77	O(H)2–NH A O(H)2–NH P	–	*2.54*	4.31	5.31	*4.70*	*4.56*	*3.51*	5.69	4.13	*2.84*
10	5.0	2.83	O(H)2–NH A O(H)4–NH P O(H)6–NH P	–	3.29	3.80	*3.71*	*3.52*	2.67	4.45	*3.17*	*2.71*	4.96
11	5.4	2.85	O(H2)–NH A O(H)3–NH P O(H)6–NH P	OH4–O(H)6	3.00	6.10	*3.65*	*3.36*	*4.65*	5.32	*3.19*	*2.70*	5.7
13	6.4	2.83	O(H)2–NH A O(H)6–NH P	–	*2.97*	6.39	*3.64*	*3.36*	*4.93*	5.29	4.37	*2.63*	4.9
15	8.5	2.86	O(H2)–NH A O(H)3–NH P O(H)4–NH P O(H)6–NH P	OH4–O(H)6	3.01	4.17	*3.71*	*3.35*	*3.19*	4.8	*2.86*	*2.52*	5.6

[a] Conformer number ranked by potential energy (AMBER*). [b] Potential energy (AMBER*). [c] Distance (Å) between the OctβMan H-4 proton and the benzene ring's centroid in receptor **1**.

shared only by the lowest-energy family of conformations. The observed receptor–ligand intermolecular NOEs were thus compared with the corresponding distance values estimated for the structures of this family, and the results are gathered in Table 3, together with the relative energies, the distances between H-4 and the benzene moiety and the detected inter- and intramolecular contacts.

From Table 3 it can easily be seen that the H-4 proton of OctβMan is unique in the complex structure, in that it is consistently pointing towards the centre of the benzene ring of the receptor, featuring distances between 2.7 and 2.8 Å. In general, for most geometries the estimated AMBER* intermolecular distances are in good agreement with the observed NOE cross-peaks. Remarkably, a hydrogen bond between the axial OH-2 of the mannosyl residue and a pyrrole or amine NH group is consistently recurrent in seven out of the eight structures, consistently with the observed selectivity of the tripodal receptor for the mannoside. The observed preference for the β-anomer over its α counterpart is easily accounted for by the lack of steric hindrance offered by the β-octyl chain to the acetal ring, with the *gem*-dimethyl substituent lying just above the α face of the mannose ring. In the case of the α-anomer, the aliphatic side chain would point towards the acetal moiety. The structure of the complex is further reinforced by additional intermolecular hydrogen bonds (six structures involving O-6, two involving O-3 and O-4 and one involving O-5), although less conserved than the OH-2/NH bond.

Comparison between the structures of complexes of receptors **1** and **2** – that is, of the structure described above with the homologous structure lacking the acetal moieties – should shed light on the binding properties exerted toward the monosaccharide ligands. Indeed, **2** has been shown to exhibit good binding affinities but a rather shallow selectivity profile toward a set of monosaccharide octyl glycosides.[6g,8] A corresponding investigation was therefore undertaken, by the same methodology, on the complex formed between **2** and OctβMan. The results are collected in Table S1 (see the Supporting Information) and reported in Figure 4.

It can easily be seen that the observed chemical shift differences follow the same trend as in the case of receptor **1**, although with smaller values. For example, although the strongest shift of the mannosyl residue is consistently observed for the H-4 proton, the CSD value is only approximately 1/3 of the value observed for receptor **1** (Figure 4, Table S1 in the Supporting Information). Furthermore, very weak intermolecular NOEs just above the noise level were observed under the same experimental conditions. By the described molecular modelling protocol, a proposed structure of the most likely interaction mode could be drawn for the corresponding complex (Figure 5). Although the relative arrangement of the partners in the complex appears to be analogous to that described for **1**, the two entities lie further apart, as can be inferred from the distance between the H-4 proton of OctβMan and the centroid of the phenyl ring (Table 4). The average distances between the protons of the sugar and the receptor are also larger than those observed in the complex of **1**, consistently with the lack of clearly observable NOEs, and detectable intermolecular hydrogen bonds are less frequent than those revealed for **1**. Thus, as a general feature, the lack of the acetal groups makes the cleft of the receptor more "wide-open" than in **1** and the glycosidic ligand consequently enjoys a

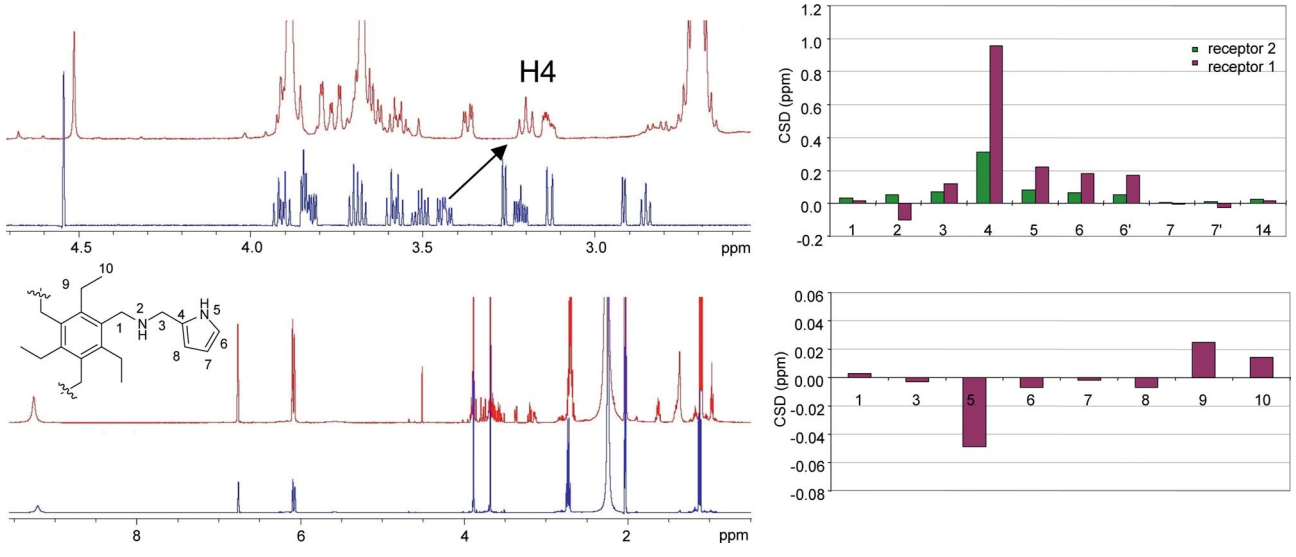

Figure 4. Left panel: 500-MHz ^{1}H NMR spectra (CD_3CN, 298 K). Top: OctβMan, neat (in blue) and in the presence of **2** (3 equiv., in red). Bottom: Compound **2** neat (printed in blue) and in the presence of OctβMan as above (printed in red). Right panel: Top: Plot of the observed CSDs of OctβMan in the presence of **1** and **2**. Bottom: Plot of the observed CSDs of **2** in the presence of OctβMan. The numbers in the graphics at the right-hand side refer to the corresponding protons in OctβMan (above) and receptor **2** (below), as shown in the scheme with the atomic numbering. The variation in the chemical shift of Man H-4 is indicated. The change in multiplicity of this signal is due to the loss of the coupling to the hydroxy proton upon binding.

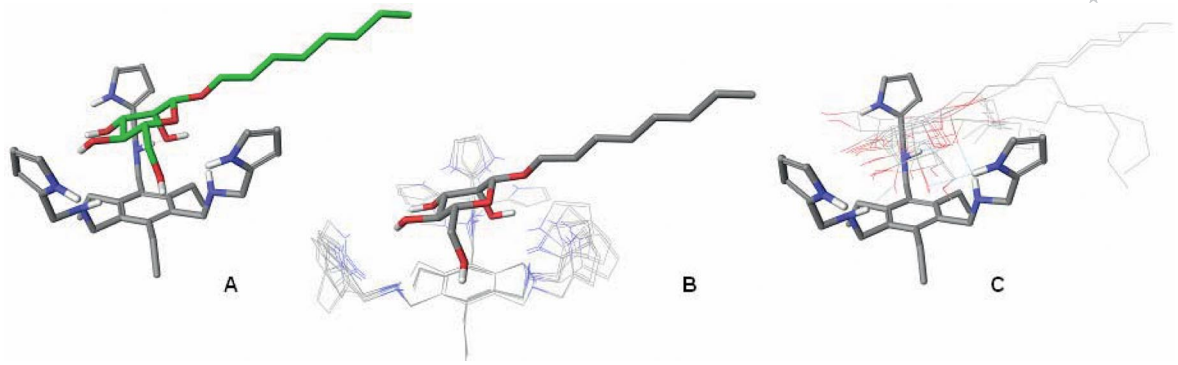

Figure 5. A) Structure of the global minimum of the 1:1 complex between **2** and OctβMan. B) Perspective from the sugar showing the orientations of the pyrrolic binding arms. C) Perspective from the receptor showing the orientations of the sugar.

larger degree of motion, resulting in looser contacts with the receptor. Furthermore, the inward orientation of the pyrrole NH group involved in the conserved H-bonding is lost in the unsubstituted receptor. Consistently with this picture, the affinity values measured for **2** towards Octα-Man and OctβMan[8] indicate weaker interaction than in the case of receptor **1**.

Table 4. Selected interatomic distances [Å] and relative energies (kJ mol^{-1}) for the most stable complexes of **2** and OctβMan. Intermolecular hydrogen bonds are reported (A: amine; P: pyrrole).

Conf.[a]	E[b]	d[c]	d[d]	H-bonds
1	0.0	3.169	4.75	OH-6/NH(A)
2	1.3	4.734	2.27	OH-6/NH(A)
				O-1/NH(A)
3	1.4	3.661	2.97	OH-2/NH(P)
				OH-2/NH(P)
				OH-3/NH(P)
				OH-3/NH(P)
4	1.5	3.202	4.8	OH-2/NH(A)
				OH-3/NH(P)
5	1.6	3.646	3.91	none
6	1.7	3.610	3.64	none
7	2.0	3.074	2.79	O-1/NH(P)
8	2.2	3.777	2.59	O-1/NH(P)

[a] Conformer number, ranked by potential energy (AMBER*). [b] Relative potential energy (AMBER*). [c] Distance between the OctβMan H-4 proton and the benzene ring centroid in receptor **2**. [d] Distance between the OctβMan H-8 proton and the pyrrole NH.

In a previous paper[8] we described the enhanced binding properties of **1** with respect to **2** in terms of the possible establishment of additional hydrogen bonding to the acetal oxygens. The structural analysis described in this work shows that the origin of the enhanced binding ability of **1** is based, rather, on the conformational features brought about by the acetal substituents, which impose a narrower size and a restricted mobility of the receptor's cleft in the bound state, thus favouring the formation of stronger hydrogen bonding to the saccharide ligand, and which appear to be particularly well suited for binding the β mannoside.

Conclusions

From a structural analysis of the complexes formed in solution between receptors **1** and **2** with OctβMan, based on NMR experimental data combined with molecular modelling calculations, it emerged that the introduction of the cyclic acetal substituents on the pyrrole units in the parent tripodal receptor induces reduced conformational freedom of the binding arms of the receptor and a narrower size of the receptor's cleft. These conformational features result in an enhanced binding ability of the receptor with respect to the parent structure, which is exerted specifically toward β-mannosides through the reinforcement of hydrogen bonding to the axial mannoside hydroxy group. The results provide an explanation of the enhanced selectivity towards mannosides observed for the acetal receptor relative to the unsubstituted progenitor. The three-dimensional models proposed for the complexes indicate that the relevant intermolecular forces involved in binding are CH–π interactions between the axial H-4 proton of OctβMan and the receptor's benzene ring, as well as hydrogen bonding between the sugar hydroxy groups and the amine/pyrrole NH groups. Additional contribution to the binding selectivity is provided by the steric hindrance caused by the alkyl chain of the glycoside, which probably hampers the α-anomer to a greater extent than the β-anomer, but affects receptor **1** much more than receptor **2**, consistently with the stricter conformational requirements of the former with respect to the latter.

This study shows that the complexation mode of the investigated tripodal receptors involves the interaction of the faces of the sugars with aromatic surfaces,[14] van der Waals interactions and hydrogen bonding through the sugar hydroxy groups,[15] as frequently found in the recognition of saccharides by lectins.[16] However, there is no evident direct parallel between the recognition of mannose by these tripodal receptors and by natural lectins, because cations (usually calcium ions) are frequently employed for mannose recognition by the biological binding site.[17] Nevertheless, knowledge of the fine details of the binding features of the tripodal receptors may allow chemical modifications en-

hancing recognition ability and selectivity. Further improvements in the receptor properties based on the findings from this work are currently under investigation.

Experimental Section

NMR Spectroscopy: NMR experiments were performed at 500 MHz with a Bruker AVANCE spectrometer, at 298 K unless otherwise stated. The experiments were performed in CD_3CN, stored over basic Al_2O_3. Experiments on the free species were recorded at 2.1 mM concentration for the glycoside (octyl β-D-mannopyranoside, OctβMan) and at 3.96 mM for receptor **1**. From the titration data,[8] for a 3:1 receptor/ligand ratio, the 1:1 complex is present in ca. 60% amount, the 2:1 complex in 20% amount and the free glycoside in 20% amount. Thus, for the detailed studies on the complexes formed in solution, the concentrations employed were 1.05 mM for the glycoside and 3.17 mM for the receptor. Analogous experiments were carried out for receptor **2**. In addition to standard 1D ^1H NMR spectra, COSY, TOCSY (35 ms mixing time) and NOESY (500 ms mixing time) experiments based on the standard BRUKER sequences[11] were also acquired, in order to assign the resonances of all the free and complexed molecular entities, as well as to obtain the intramolecular and intermolecular distances. For NOESY, we chose this relatively long mixing time because we were dealing with small molecules (292 and 829 Da), in low-viscosity solvents, with T_1 values of around 0.5–1.5 s. We were far from the spin diffusion limit, within the positive NOE range, and so the possibilities of having confusing spin-diffusion effects were negligible. With this mixing time we obtained clear and measurable intermolecular NOEs, certainly direct effects, that helped us to deduce the geometry of the complex.

Molecular Modelling: The structures of OctβMan and receptors **1** and **2** were built with use of Maestro[12] and minimized by use of conjugate gradients with the AMBER* force field[13] and a dielectric constant of 37.5 Debyes for acetonitrile. Once the optimum geometries had been achieved, a conformational search protocol was adopted, with the same force field and conditions. Firstly the receptor alone was subjected to the search, with use of a Monte Carlo torsional sampling (MCMM) with the default settings. The best structure obtained from this calculation in terms of energy was chosen, and the mannoside was then manually docked within its cavity and further minimized. The complex was found to be stable, because the sugar remained inside the receptor cleft on energy minimization. This local minimum was thus taken as the starting geometry for an additional conformational search process, with no constraints, with the same settings as before. Twenty geometries of the complex, within 10 kJ mol^{-1} of the global minimum, were chosen for further analysis. The obtained structures were classified into three clusters, differing in the orientation of the saccharide with respect to the receptor. In the first one (A), the sugar ring was oriented with H-4 pointing towards the benzene ring of the scaffold. In the second (B), the sugar ring occupied an orientation opposite to that of A, with the H-4 pointing away from the benzene ring. In the third (C), the sugar ring occupied a position perpendicular to the benzene ring. The lowest-energy structure corresponded to family A (Figure 3), which included seven geometries featuring slightly different orientations of the sugar and of the binding arms of the tripodal receptor. These geometries were considered to correspond to the most likely NMR-based experimental solution and were further explored. Because of the motion features for the formed complex, a realistic full quantitative analysis of the NOEs was not performed. Direct comparison between the estimated intermolecular distances for a "fixed" complex with the experimentally measured NOEs was a solid base for deducing the structure of the complex.

Supporting Information (see also the footnote on the first page of this article): Table of NMR parameters for receptor **2**.

Acknowledgments

This work was supported by a grant from the Ministry of Science and Innovation of Spain (CTQ2006-10874-C02-01 and CTQ2009-8536) and by a European Cooperation in the Field of Science and Technology (COST) action.

[1] H.-J. Gabius, H.-C. Siebert, S. André, J. Jiménez-Barbero, H. Rüdiger, *ChemBioChem* **2004**, *5*, 740–764.
[2] C. R. Bertozzi, L. L. Kiessling, *Science* **2001**, *291*, 2357–2364.
[3] *The Sugar Code. Fundamentals of glycosciences* (Ed.: H.-G. Gabius), Wiley-VCH, Weinheim, **2009**.
[4] a) M. C. Fernández-Alonso, F. J. Cañada, J. Jiménez-Barbero, G. Cuevas, *J. Am. Chem. Soc.* **2005**, *127*, 7379–7386; b) S. Vandenbussche, D. Díaz, M. C. Fernández-Alonso, W. Pan, S. P. Vincent, G. Cuevas, F. J. Cañada, J. Jiménez-Barbero, K. Bartik, *Chem. Eur. J.* **2008**, *14*, 7570–7578; c) Z. R. Laughrey, S. E. Kiehna, A. J. Riemen, M. L. Waters, *J. Am. Chem. Soc.* **2008**, *130*, 14625–14633.
[5] H. Kogelberg, D. Solís, J. Jiménez-Barbero, *Curr. Opin. Struct. Biol.* **2003**, *13*, 646–653.
[6] For recent reviews and developments in artificial lectins, see: a) Y. Ferrand, M. P. Crump, A. P. Davis, *Science* **2007**, *318*, 619–622; b) E. Klein, Y. Ferrand, N. P. Barwell, A. P. Davis, *Angew. Chem. Int. Ed.* **2008**, *47*, 2693–2696; c) P. B. Palde, P. C. Gareiss, B. L. Miller, *J. Am. Chem. Soc.* **2008**, *130*, 9566–9573; d) C. He, Z. H. Lin, Z. He, C. Y. Duan, C. H. Xu, Z. M. Wang, C. H. Yan, *Angew. Chem. Int. Ed.* **2008**, *47*, 877–881; e) M. Waki, H. Abe, M. Inouye, *Angew. Chem. Int. Ed.* **2007**, *46*, 3059–3061; f) T. Reenberg, N. Nyberg, J. O. Duus, J. L. J. van Dongen, M. Meldal, *Eur. J. Org. Chem.* **2007**, 5003–5009; g) C. Nativi, M. Cacciarini, O. Francesconi, A. Vacca, G. Moneti, A. Ienco, S. Roelens, *J. Am. Chem. Soc.* **2007**, *129*, 4377–4385; h) M. Mazik, M. Kuschel, *Chem. Eur. J.* **2008**, *14*, 2405–2419; i) M. Mazik, *Chem. Soc. Rev.* **2009**, *38*, 935–956; j) S. Kubik, *Angew. Chem. Int. Ed.* **2009**, *48*, 1722–1725.
[7] For some additional recent leading references in artificial lectins and their recognition abilities, see: a) C. Li, G.-T. Wang, H.-P. Yi, X.-K. Jiang, Z.-T. Li, R.-X. Wang, *Org. Lett.* **2007**, *9*, 1797–1800; b) J. Bitta, S. Kubik, *Org. Lett.* **2001**, *3*, 2637–2640; c) Y.-H. Kim, J.-I. Hong, *Angew. Chem. Int. Ed.* **2002**, *41*, 2947–2950; d) M. Segura, B. Bricoli, A. Casnati, E. M. Muñoz, F. Sansone, R. Ungaro, C. Vicent, *J. Org. Chem.* **2003**, *68*, 6296–6303; e) M. Dukh, D. Šaman, K. Lang, V. Pouzar, I. Černý, P. Drašar, V. Král, *Org. Biomol. Chem.* **2003**, *1*, 3458–3463; f) A. Vacca, C. Nativi, M. Cacciarini, R. Pergoli, S. Roelens, *J. Am. Chem. Soc.* **2004**, *126*, 16456–16465; g) S. Roelens, A. Vacca, C. Venturi, *Chem. Eur. J.* **2009**, *15*, 2635–2644; h) Y. Ferrand, E. Klein, N. P. Barwell, M. P. Crump, J. Jiménez-Barbero, C. Vicent, G. J. Boons, S. Ingale, A. P. Davis, *Angew. Chem. Int. Ed.* **2009**, *48*, 1775–1779; i) O. Francesconi, A. Ienco, G. Moneti, C. Nativi, S. Roelens, *Angew. Chem. Int. Ed.* **2006**, *45*, 6693–6696, and references therein.
[8] C. Nativi, M. Cacciarini, O. Francesconi, G. Moneti, S. Roelens, *Org. Lett.* **2007**, *9*,4685–4688.
[9] a) See, for instance: W. Lu, L.-H. Zhang, X.-S. Ye, J. Su, Z. Yu, *Tetrahedron* **2006**, *62*, 1806–1816; b) H. Abe, Y. Aoyagi, M. Inouye, *Org. Lett.* **2005**, *7*, 59–61; c) J.-M. Fang, S. Selvi, J.-H. Liao, Z. Slanina, C.-T-Chen, P.-T. Chou, *J. Am. Chem. Soc.* **2004**, *126*, 3559–3566.

[10] D. Neuhaus, M. P. Williamson (Eds.), *The Nuclear Overhauser Effect in Structural and Conformational Analysis*, VCH Publishers, New York, **1989**.
[11] For a description of NMR experiments for free and bound carbohydrate molecules, see: *NMR Spectroscopy of Glycoconjugates* (Eds.: J. Jiménez-Barbero, T. Peters), Wiley-VCH, Weinheim, **2002**.
[12] *Maestro*, A powerful, all-purpose molecular modeling environment, version 8.5, Schrödinger, LLC, New York, NY **2008**.
[13] D. A. Case, T. E. Cheatham III, T. Darden, H. Gohlke, R. Luo, K. M. Merz Jr., A. Onufriev, C. Simmerling, B. Wang, R. J. Woods, *J. Comput. Chem.* **2005**, *26*, 1668–1687.
[14] a) M. I. Chávez, C. Andreu, P. Vidal, N. Aboitiz, F. Freire, P. Groves, J. L. Asensio, G. Asensio, M. Muraki, F. J. Cañada, J. Jiménez-Barbero, *Chem. Eur. J.* **2005**, *11*, 7060–7074; b) J. L. Asensio, H.-C. Siebert, C. W. von Der Lieth, J. Laynez, M. Bruix, U. M. Soedjanaamadja, J. J. Beintema, F. J. Cañada, H.-J. Gabius, J. Jiménez-Barbero, *Proteins* **2000**, *40*, 218–236.
[15] H.-C. Siebert, S. André, J. L. Asensio, F. J. Cañada, X. Dong, J. F. Espinosa, M. Frank, M. Gilleron, H. Kaltner, T. Kozár, N. V. Bovin, C. W. von Der Lieth, J. F. Vliegenthart, J. Jiménez-Barbero, H.-J. Gabius, *ChemBioChem* **2000**, *1*, 181–195.
[16] a) A. García-Herrero, E. Montero, J. L. Muñoz, J. F. Espinosa, A. Vián, J. L. García, J. L. Asensio, F. J. Cañada, J. Jiménez-Barbero, *J. Am. Chem. Soc.* **2002**, *124*, 4804–4810; b) J. F. Espinosa, J. L. Asensio, J. L. García, J. Laynez, M. Bruix, C. Wright, H.-C. Siebert, H.-G. Gabius, F. J. Cañada, J. Jiménez-Barbero, *Eur. J. Biochem.* **2000**, *267*, 3965–3978.
[17] H. Feinberg, D. A. Mitchell, K. Drickamer, W. I. Weis, *Science* **2001**, *294*, 2163–2166.

Received: September 8, 2009
Published Online: November 20, 2009

